Biochemistry

pubs.acs.org/biochemistry

From the Bench

Capturing Membrane Protein Ribosome Nascent Chain Complexes in a Native-like Environment for Co-translational Studies

Grant A. Pellowe, Heather E. Findlay, Karen Lee, Tim M. Gemeinhardt, Laura R. Blackholly, Eamonn Reading,* and Paula J. Booth*

Cite This: *Biochemistry* 2020, 59, 2764–2775

Read Online

ACCESS | Metrics & More | Article Recommendations | Supporting Information

ABSTRACT: Co-translational folding studies of membrane proteins lag behind cytosolic protein investigations largely due to the technical difficulty in maintaining membrane lipid environments for correct protein folding. Stalled ribosome-bound nascent chain complexes (RNCs) can give snapshots of a nascent protein chain as it emerges from the ribosome during biosynthesis. Here, we demonstrate how SecM-facilitated nascent chain stalling and native nanodisc technologies can be exploited to capture *in vivo*-generated membrane protein RNCs within their native lipid compositions. We reveal that a polytopic membrane protein can be successfully stalled at various stages during its synthesis and the resulting RNC extracted within either detergent micelles or diisobutylene−maleic acid co-polymer native nanodiscs. Our approaches offer tractable solutions for the structural and biophysical interrogation of nascent membrane proteins of specified lengths, as the elongating nascent chain emerges from the ribosome and inserts into its native lipid milieu.

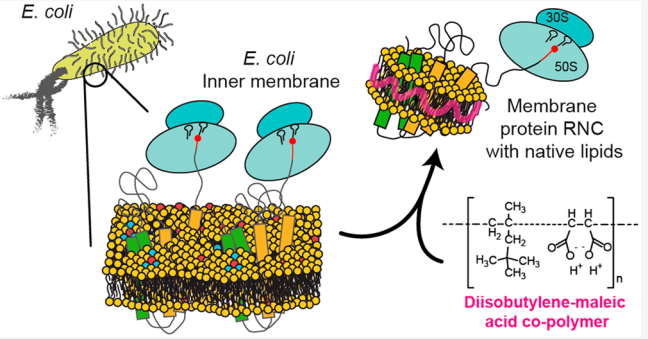

Most proteins begin to fold as they are translated unidirectionally from N- to C-termini by the ribosome. A significant drawback to much existing research into folding mechanisms is the study of full-length, isolated proteins that are unrepresentative of this co-translational cellular biosynthesis. A key advance has been the development of ribosome nascent chain (RNC) preparations in which elongating nascent chains are stalled at various points, so that biophysical methods can be used to probe the structures of specified length chains attached to ribosomes.[1−9] Typically, the *Escherichia coli* arrest sequence SecM is employed to halt translation.[2,9,10] Stalling translation, as well as truncating nascent chains, has proven to be instrumental in membrane protein insertion studies, but as yet, no membrane protein RNCs have been isolated directly from cells in their native lipid environments, which hinders detailed molecular mechanistic and structural investigations.

Co-translational folding of α-helical transmembrane (TM) proteins is often assisted by a membrane insertase apparatus, such as the *E. coli* SecYEG translocon. SecYEG forms the basis of a holotranslocon (HTL), along with co-proteins SecDF and insertase YidC.[11] An emerging nascent chain is delivered to the SecYEG translocon by the signal recognition particle (SRP). Lipid interactions influence membrane insertion,[12,13] with lipid headgroup charge and interactions with the nascent chain affecting TM insertion efficiency and topology.[14] The bulk properties of the lipid bilayer, such as its lateral pressure and hydrophobic thickness, also likely impact membrane protein insertion and folding.[12] Thus, the cell membrane "arena" required for membrane protein folding adds increasing complexity to the already intricate co-translational folding pathway of proteins.

Membrane protein co-translational folding and insertion have largely been studied using *in vitro* transcription/translation (IVTT). This *in vitro* approach enables control of protein translation within simplified cell and membrane extracts, or purified components such as the PURExpress system[15] and synthetic lipid mixtures. Assorted investigations of the inserted state have been undertaken using biochemical assays such as epitope binding, limited proteolysis, and chemical cross-linking.[16−22] Moreover, structure formation during co-translational folding has been probed by infrared spectroscopy.[21] These studies have led to exceptional insight into the co-translational insertion of membrane proteins; however, these translation systems often give low yields and are expensive.

The use of the *E. coli* SecM stalling sequence, found in nature to regulate the translation rate of higher-order proteins during co-translational folding,[23,24] is perhaps the most

Received: May 19, 2020
Revised: July 2, 2020
Published: July 6, 2020

https://dx.doi.org/10.1021/acs.biochem.0c00423
Biochemistry 2020, 59, 2764–2775

common method for RNC generation. In wild-type (WT) SecM, a proline at position 166 alters the geometry of the peptidyl transferase center (PTC) preventing the formation of the ester linkage, resulting in the subsequent stalling of the ribosome along the mRNA.[9,24,25] Insertion of a SecM sequence downstream of a nascent chain allows RNCs to be generated both *in vitro* and *in vivo*,[23] thus trapping a polypeptide chain at a specified "length". In addition, SecM has been used to give a measure of the force exerted on a TM helix during membrane insertion,[16,17,26] and an amino acid hydrophobicity scale has been derived from apparent free energies of TM insertion.[27] Other stalling sequences exist, such as the TnaC stalling peptide that makes extensive contacts with the majority of the ribosome exit tunnel,[6] rather than altering the PTC. Although these stalling methods have proven to be highly informative, we are still some way from understanding the molecular details of membrane protein co-translational folding, with our molecular and mechanistic knowledge currently deriving from refolding studies of full-length isolated nascent chains.[28]

For water-soluble proteins, the production and purification of high yields of homogeneous RNCs samples have enabled structural snapshots to be obtained at different nascent chain lengths, in particular by cryo-electron microscopy (cryoEM) analysis.[1−3] Moreover, it has been shown that RNCs are suited for advanced biophysical analysis, impressive examples being the use of solution-state nuclear magnetic resonance (NMR) to decipher a nascent chain structural ensemble[1−3,9] and mechanical force manipulation for stability assessment of the nascent chain fold.[29,30]

Membrane protein RNCs are considerably more challenging to isolate than those for water-soluble proteins, as they are complicated by the requirement of a lipid membrane. Nevertheless, notable achievements have been made in the cryoEM structural characterization of membrane protein RNCs. For example, Beckmann et al. found, at high resolution, that interaction of a TM nascent chain with SecY can cause opening of its channel, likely to facilitate its insertion into the membrane. To achieve this interaction, they used detergent-solubilized RNCs that were then subsequently reconstituted with SecY-containing membrane scaffold protein (MSP)-based nanodiscs consisting of non-native lipid DMPC.[4,5] Membrane mimetics such as these provide a lipid bilayer but lack the native lipid composition and, therefore, may not truly represent its functional environment.

To improve this, polymer scaffolds have recently been used as a method to directly solubilize MPs within nanodiscs of their native lipid surround (so-called "native" nanodiscs), thus removing the requirement for detergent purification and reconstitution. The most widely used scaffold is the styrene-maleic acid (SMA) co-polymer. However, when considering the preparation and analysis of ribosome-containing samples, the SMA co-polymer has its disadvantages: SMA contains a large styrene aromatic ring that contributes to high-absorption spectra in the low-ultraviolet region, which makes concentration and purity analysis of RNCs using A_{280}/A_{260} difficult.[31,32] SMA is also less tolerant to divalent cations, with the precipitation of the polymer occurring at Mg^{2+} concentrations of >5 mM.[33] An *E. coli* 70S ribosome contains more than 170 Mg^{2+} atoms, with the loss of bound Mg^{2+} leading to 70S dissociation and degradation.[34] Therefore, to maintain 70S integrity, an *in vitro* Mg^{2+} concentration of >5 mM is typically required, making SMA unsuitable for RNC study. To circumvent these spectroscopic and divalent cation issues, the recently utilized diisobutylene-maleic acid (DIBMA) co-polymer was selected.[31] Its polymer structure contains an aliphatic diisobutylene moiety instead of the aromatic styrene component found within SMA. This allows for spectroscopic study as the styrene component that absorbed strongly within the range of 260−280 nm has been removed. Importantly, DIBMA also has a proven tolerance to high concentrations of divalent cations (≤20 mM for Mg^{2+} and ≤35 mM for Ca^{2+}),[31,35] making it a suitable candidate for ribosome study. Both DIBMA and SMA co-polymers produce thermostable MP nanodiscs, but DIBMA has a weaker impact on the acyl chain order and lipid phase in solubilized membranes than SMA, maintaining a nearer physiological membrane environment.[31]

In view of the importance of lipid composition and membrane properties in defining the behavior of membrane proteins, we have developed an approach to extracting RNCs directly from their cellular membrane. We present a strategy for producing high yields of homogeneous polytopic membrane protein RNCs within their native lipid environments. Membrane protein RNCs are isolated from native membranes using DIBMA co-polymer native nanodisc technology.[33,36,37] Overall, our approach enables the structural and biochemical interrogation of cellular co-translational membrane protein translation and folding within a more physiological environment than is currently possible with existing *in vitro* or reconstituted systems.

MATERIALS AND METHODS

Plasmid Construction. His_6-GlpG-SecM plasmids were constructed for GlpG RNC overexpression. pET28a was linearized with NdeI and XhoI restriction enzymes (New England Biolabs). The glpg gene (subcloned from Harris et al.[21]) and a 44-amino acid sequence motif encoding both the SecM arrest motif and additional amino acids (subcloned from Rutkowska et al.[9]) were amplified and cloned simultaneously into the linearized pET28a vector using In-Fusion HD cloning (Takara Bio). The resulting pET28a-His_6-GlpG-SecM vector was then used in subsequent deletion cloning reactions to generate constructs of different GlpG "lengths" using the Q5 site-directed mutagenesis kit (New England Biolabs). A pET28a-His_6-GlpG plasmid was also generated for overexpression of His_6-GlpG without the linker-SecM sequence using the same procedures.

To substitute the WT SecM sequence for the arrest-enhanced (AE1) SecM sequence, primers were designed for the AE1 sequence based on Cymer et al.,[26] and polymerase chain reaction was carried out using the Q5 site-directed mutagenesis kit (New England Biolabs) on each RNC vector.

GlpG-RNC Growth in BL21 (DE3). N-Terminal His_6-tagged GlpG constructs were truncated after two, four, and six TM helices using a WT SecM sequence, cloned into the pET28a expression vector, and transformed into *E. coli* strain BL21 (DE3). The following growth conditions are based on NMR protocols yielding large quantities of highly occupied RNCs,[2] which provide a maximal number of ribosomes ready for NC expression and are amenable to isotopic or selective labeling of the NCs.

Overnight LB cultures grown at 37 °C were used to seed 6 L of MDG {phosphate (M), aspartic acid (D), glucose (G) media [1× MDG salts (25 mM Na_2HPO_4, 25 mM KH_2PO_4, 50 mM NH_4Cl, and 5 mM Na_2SO_4), 0.2% (w/v) L-aspartic acid (pH 7.0), 0.4% (w/v) D-glucose, 2 mM $MgSO_4$, and 0.2×

https://dx.doi.org/10.1021/acs.biochem.0c00423
Biochemistry 2020, 59, 2764−2775

trace metals, which were subsequently grown to saturation at 30 °C with shaking at 220 rpm]}. Cells were harvested by centrifugation before suspension of an equal volume of enhanced M9 media [1× EM9 salts (7.1 g/L Na_2HPO_4, 3.4 g/L KH_2PO_4, and 0.58 g/L NaCl adjusted to pH 8.0−8.2), 0.4% (w/v) D-glucose, 5 mM $MgSO_4$, 200 μM $CaCl_2$, 0.25× trace metals, and 0.1% (w/v) NH_4Cl] for induction. Trace metals were mixed as a 1000× stock containing 5 g/L EDTA, 0.83 g/L $FeCl_3·6H_2O$, 0.05 g/L $ZnCl_2$, 0.01 g/L $CuCl_2$, 0.01 g/L $CoCl_2·6H_2O$, 0.01 g/L H_3BO_3, and 1.6 g/L $MnCl_2·6H_2O$ (pH 7.0). All media were supplemented with 30 μg/mL kanamycin. Cells were induced for protein production using 1 mM isopropyl β-D-1-thiogalactopyranoside (IPTG) for 1.5−2 h at 30 °C before being washed with ice-cold PBS, harvested, and resuspended in lysis buffer [50 mM HEPES-KOH (pH 7.5), 1 M KOAc, 12 mM $Mg(OAc)_2$, 5% (v/v) glycerol, 5 mM EDTA, 2 mM 2-mercaptoethanol, 1 mM phenylmethanesulfonyl (PMSF), 250 μg/mL chloramphenicol, and cOmplete EDTA-free protease inhibitor tablet (Roche)] with 1% lysozyme and RNase-free DNase I (NEB) and stored at −20 °C or flash-frozen and stored at −70 °C as "pellets" for cryo-milling.

For biotinylated RNC-GlpG, constructs with an N-terminal Avi tag were co-transformed with pBirAcm (Avidity), maintained by 10 μg/mL chloramphenicol, to express BirA. Cells were also grown to saturation in MDG media. However, to the enhanced M9 media was added 50 μM D-biotin dissolved in 10 mM bicine buffer (pH 8.3). The two plasmids were both induced using 1 mM IPTG and grown as described above, producing biotinylated RNC-GlpG constructs.

Alternatively, BL21-AI cells can be grown and RNCs expressed in Luria-Bertani or 2-YT medium. For these, 100 mL overnight cultures were seeded as described above, and cells grown at 37 °C until an OD_{600} of 1.8 was reached. Cultures were cooled to 30 °C and induced with 1 mM IPTG and 0.1% L-arabinose for 1 h. Cells were washed and harvested as described above.

DIBMA Preparation. The diisobutylene/maleic acid copolymer (DIBMA) was precipitated out of a Sokalan CP9 solution (BASF) with 0.6 V of 4 M HCl. The solid was centrifuged at 17000*g* for 15 min and washed with doubly distilled H_2O (ddH_2O). This was repeated four times; 1.2 V of 4 M NaOH was used to solubilize the solid, before repeating the precipitation and washing steps described above. The wet pellet was then lyophilized for 72 h to produce the pure DIBMA polymer.[38,39]

The polymer was used to produce 20% (w/v) stocks in 2 M NaOH. Base was then added dropwise to carefully dissolve the solid and adjust the pH to 8.0. The concentration of the polymer solution was checked using a Reichert AR200 digital refractometer with a dn/dc of 1.346 M^{-1}.[31] The 20% stock was used to produce 2.5% stocks in the necessary buffer for the solubilization of *E. coli* membranes.

Lyophilized DIBMA stocks were quality checked[39] using a Shimadzu IR Affinity-1s or a PerkinElmer Spectrum Two FTIR instrument, scanned across a complete wavenumber range of 4000−400 cm^{-1}, with 16 scans to measure transmittance (Figure S3a). In particular, the carboxylate (1705 cm^{-1}) and anhydride (1775 cm^{-1}) bands were checked to ensure that our treatment of the polymer with strong acids did not result in a condensation of the anhydride ring, which would result in a significantly reduced solubilization efficiency.

Purification of DDM and DIBMA GlpG-RNCs. The cell lysis buffer described above and all subsequent RNC preparation buffers were prepared using RNase-free water to prevent the degradation of the rRNA content in our RNCs. This was prepared by incubating ddH_2O with 0.1% diethyl pyrocarbonate (DEPC) to inactivate any RNase, prior to autoclaving that facilitated the removal of DEPC by decomposition into CO_2 and ethanol.

Cells were defrosted slowly and lysed using sonication, or cryo-milled in a Spex 6875 Freezer/Mill High Capacity Cryogenic Grinder using 15 cycles of 15 cps and allowed to thaw on ice. The cell debris was removed by centrifugation at 20000*g* for 45 min at 4 °C. This was repeated in fresh tubes if the resulting supernatant did not clear. The supernatant was then spun at 125000*g* for 30 min at 4 °C to harvest cell membranes with associated ribosomes. The crude membrane pellet was resuspended at concentrations of 25−50 mg/mL in washing buffer [50 mM HEPES-KOH (pH 7.5), 500 mM KOAc, 12 mM $Mg(OAc)_2$, 5% (v/v) glycerol, 2 mM 2-mercaptoethanol, and 1 mM PMSF] aided by homogenization. To this suspension, 1% dodecyl maltoside (DDM) or 2.5% DIBMA (pH adjusted to 8.0) was added, and the mixture solubilized for 2 h at 4 °C or for 1 h at 25 °C, respectively. The solubilized membranes were spun at 125000*g*, and the supernatant was filtered before purification using an AKTA Pure system.

DDM-solubilized ribosomes carrying the nascent chain were purified using an AKTA Pure purification system. First, samples were separated by affinity chromatography using a HisTrap Nickel column. The column was washed with 5 column volumes of washing buffer containing 0.1% DDM. RNCs were passed over the column to allow binding. The column was washed with 30 mL of washing buffer with 20 mM imidazole with 0.1% DDM. RNCs were then eluted in washing buffer containing 500 mM imidazole and directly loaded onto a 16/60 HiPrep Sephacryl S-400 HR size-exclusion column pre-equilibrated with Tico size-exclusion buffer [10 mM HEPES-KOH (pH 7.5), 30 mM NH_3Cl, 12 mM $Mg(OAc)_2$, 5% (v/v) glycerol, 1 mM EDTA, 2 mM 2-mercaptoethanol, and 0.1 mM PMSF] containing 0.1% DDM. According to the manufacturer's specifications, the separation range of the Sephacryl S-400 column is 20 kDa to 8 MDa.

DIBMA-solubilized ribosomes with native membranes were first bound overnight at 4 °C to superaffinity Ni-NTA beads (Generon) pre-equilibrated with washing buffer before further cleanup using AKTA Pure. The supernatant containing unbound species was discarded, and beads were washed with 20 mM imidazole in washing buffer, before elution in 5 mL of washing buffer containing 500 mM imidazole. DDM was not present in any of these buffers. The eluate was subsequently concentrated to 2 mL using a 100 or 300 kDa concentrator and loaded directly onto the 16/60 HiPrep Sephacryl S-400 HR size-exclusion column pre-equilibrated with Tico size-exclusion buffer containing 0.2 M L-arginine. The left-hand side of the elution peak, previously shown to contain the highest proportion of 70S ribosomes with the nascent chain,[40] was taken and concentrated, and buffer exchange was carried out in a 100 or 300 kDa molecular weight cutoff spin concentrator and passed over a PD10 G25-superdex column, which facilitated the removal of arginine.

The RNC absorbance at 260 and 280 nm was monitored to evaluate the 70S content and its homogeneity using the OD_{260}/OD_{280} ratio (expected range of 1.9−2.0; 1 OD_{260} = 24

https://dx.doi.org/10.1021/acs.biochem.0c00423
Biochemistry 2020, 59, 2764−2775

pmol/mL[41])]. The samples were flash-frozen after purification; the samples were stable after freezing and thawing and observed to be homogeneous.

Western Blotting Analysis. To assess the RNC integrity, 1−2 pmol samples were run on 12% (w/v) NuPAGE gels at neutral pH and with a sample dye at pH 5.7 [30% glycerol, 0.25 M Bis-Tris (pH 5.7), 0.8% DTT, 8% SDS, and bromophenol blue] to maintain the ester bond between the tRNA and the nascent chain. DIBMA samples were boiled at 95 °C for 10 min prior to gel loading, and insoluble DIBMA material was spun out for 2 min at the maximum microfuge speed. To obtain the released forms of the nascent chain, the RNC samples were treated with 10 μg of RNase A to digest the rRNA (at room temperature for 5 min). The samples were analyzed by Western blotting using anti-histidine and streptavidin-HRP conjugate antibodies. For SecYEG Western blotting, an anti-SecY mouse antibody was used with an anti-mouse HRP secondary antibody. ImageJ[42] was used for densitometry analysis where necessary. Novex Sharp pre-stained protein ladder (Invitrogen) or PageRuler Plus prestained ladder (ThermoFisher) molecular weight markers were used.

It is worth noting that DIBMA, and other polymers, are prone to smearing when they are run on sodium dodecyl sulfate−polyacrylamide gel electrophoresis (SDS−PAGE) gels and transferred to nitrocellulose. To allow the proteinaceous component to enter the acrylamide, it was necessary to boil the samples at 95 °C for 10 min to encourage denaturation before gel loading. The low-pH nature of the SDS loading dye precipitated out the DIBMA as expected.

RNC occupancy was achieved through the botting of full-length GlpG standards to produce a standard curve of blot intensity against picomoles of GlpG (Figure S5c), against a known concentration of RNC based on the rRNA-determined concentrations where 1 OD_{260} = 24 pmol/mL.[2]

Dynamic Light Scattering. Dynamic light scattering for DIBMA RNCs was carried out in Tico buffer in particle size mode on a Malvern ZetaSizer machine.

Sucrose Gradient Purifications. Samples to be purified with a sucrose density gradient were solubilized and bound/eluted to superaffinity Ni-NTA resin as described above. Eluates were buffer exchanged out of imidazole using 100 kDa cutoff concentrators and PD10 columns equilibrated with washing buffer or pelleted at 117000*g* for 4 h and suspended in a suitable volume of washing buffer. Sucrose gradients were prepared with five steps of 5%, 10%, 20%, 30%, and 40% sucrose in washing buffer containing no glycerol. The sample was layered on top and centrifuged at 202000*g* in a Beckmann SW40 rotor for 16 h at 4 °C before 1 mL or 500 μL fractions were taken for analysis.

Thin-Layer Chromatography Analysis of DIBMA-Solubilized Samples. To extract lipids of the native membrane RNCs, a modified Folch method was used.[43] A 500 μL DIBMA-solubilized sample was added to 1.1 mL of a 10:23:1 (v/v) $CHCl_3$/MeOH/1 M Tris (pH 8.0) solvent and mixed well for 1 h at 25 °C. Phase separation was then achieved by adding 1 mL of a 1:1 $ChCl_3$/1 M Tris (pH 8.0) solvent; the mixture was vortexed, and each phase was allowed to separate at room temperature. The upper aqueous phase was removed, and the organic layer washed with ion switch buffer [50 mM Tris, 100 mM NaCl, and 100 mM EDTA (pH 8.0)] before being dried under a stream of nitrogen and suspended in $CHCl_3$ to the desired TLC concentration.

HPTLC silica gel TLC plates were run as described in ref 44 and washed in a 1:1 $CHCl_3$/MeOH solvent before being air-dried. The plate was immersed in 2.3% boric acid in EtOH, air-dried, and baked at 100 °C for 15 min. One microgram of 18:1 1,2-dioleoyl-*sn*-glycero-3-phosphoethanolamine (DOPE), 18:1 1,2-dioleoyl-*sn*-glycero-3-phospho-(1′-*rac*-glycerol) (DOPG), and *E. coli* cardiolipin (all from Avanti) were spotted along with the extract samples, and plates were run in a 65:25:4 $CHCl_3$/MeOH/CH_3COOH solvent to achieve good head-group separation of the lipids. The plate was immersed in a copper char solution (10% $CuSO_4$ and 8% H_3PO_4) before air drying and further charring at 145 °C for 15 min. Plates were imaged using blue fluorescence once they had cooled. Alternatively, the dried plate was stained with iodine vapor or sprayed with a molybdenum blue stain (commercial Dittmer-Lester stain[45]) to specifically detect phospholipid. ImageJ[42] was used for densitometry analysis, where the raw spot intensity was converted to mole fraction, and the percentage of total lipid composition was plotted with SD for at least three biological repeats (new growth and preparation of RNCs, lipid extraction, and running of TLC plates).

Growth and Preparation of Full-Length WT N_{His}-GlpG and GlpG-MycHis$_6$. pET28a-His_6-GlpG and pET28a-GlpG-$MycHis_6$ plasmids were transformed into C43 *E. coli* cells (Sigma-Aldrich). Seven milliliters of an overnight-saturated culture was added to 1 L of LB culture, both with 30 μg/mL kanamycin. These cultures were grown at 37 °C until an OD of 0.6−0.8 was achieved. The cultures were then cooled to 16 °C, induced with 1 mM IPTG, and left overnight before the cells were harvested. The cells were washed with PBS and either stored at −80 °C or used immediately.

Cell pellets were thawed and resuspended in buffer A [300 mM sodium chloride and 20 mM 2-amino-2-hydroxymethyl-propane-1,3-diol (Tris) (pH 7.4) at room temperature] supplemented with a cOmplete protease inhibitor tablet (Roche), PMSF, Benzonase nuclease, and 5 mM β-mercaptoethanol (β-ME).

The cell suspension was passed twice through a micro-fluidizer (Constant Systems) at 25000 psi. Insoluble material was pelleted by centrifugation twice at 20000*g* for 25 min at 4 °C. Membranes were pelleted by centrifugation at 150000*g* for 1.5 h at 4 °C.

Membranes were resuspended at a concentration of 40 mg/mL in ice-cold buffer B [500 mM sodium chloride, 10% glycerol, and 50 mM Tris (pH 7.4) at room temperature] supplemented with a cOmplete protease inhibitor tablet (Roche) and PMSF and homogenized using a Potter-Elvehjem Teflon pestle and glass tube.

DDM was added to the suspension at a final concentration of 1% (w/v) to solubilize the membranes. The cell suspension with DDM was incubated overnight with gentle agitation at 4 °C, followed by centrifugation at 100000*g* for 1 h at 4 °C.

The supernatant was then filtered before being loaded onto a 1 mL HisTrap column (GE Healthcare) equilibrated in buffer B [500 mM sodium chloride, 20 mM imidazole, 10% (v/v) glycerol, 50 mM Tris (pH 7.4) at room temperature, and 0.025% (w/v) DDM].

The column was washed with 10 mL of buffer B and then 20 mL of 5% buffer C [500 mM sodium chloride, 500 mM imidazole, 10% (v/v) glycerol, 50 mM Tris (pH 7.4) at room temperature, and 0.025% (w/v) DDM].

https://dx.doi.org/10.1021/acs.biochem.0c00423
Biochemistry 2020, 59, 2764−2775

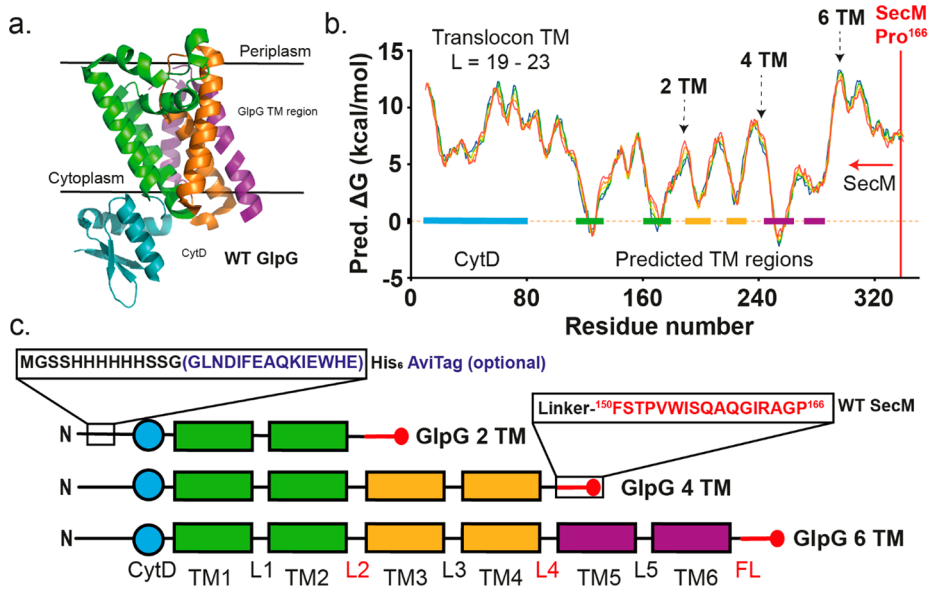

Figure 1. Construct design of GlpG RNCs at different co-translational "intermediates". (a) PDB structure of WT GlpG: TM region, with helices 1 and 2 colored green, helices 3 and 4 colored orange, and helices 5 and 6 colored purple (PDB entry 2XTV[49]) and the cytoplasmic domain (CytD) colored blue (PDB entry 2LEP[48]). (b) MPEx[27] translocon TM predicted hydropathy plot for full-length GlpG with linker-WT SecM. A sliding scale length (L) of 19−23 amino acids was used for MPEx hydropathy prediction. Arrows depict the position chosen for the 3′ cloning of linker-WT SecM. This provides 44 amino acid residues between a stable TM helix and the SecM Pro[166] stalling residue. (c) Construct design for RNC truncations of GlpG. WT SecM was cloned to the C-terminus of each construct (red). A six-histidine tag was cloned to the N-terminus of the construct. An additional Avi tag (purple) could also be cloned and successfully utilized for *in vivo* biotinylation if desired (see the Supporting Information). The color scheme for GlpG constructs is consistent with panel a.

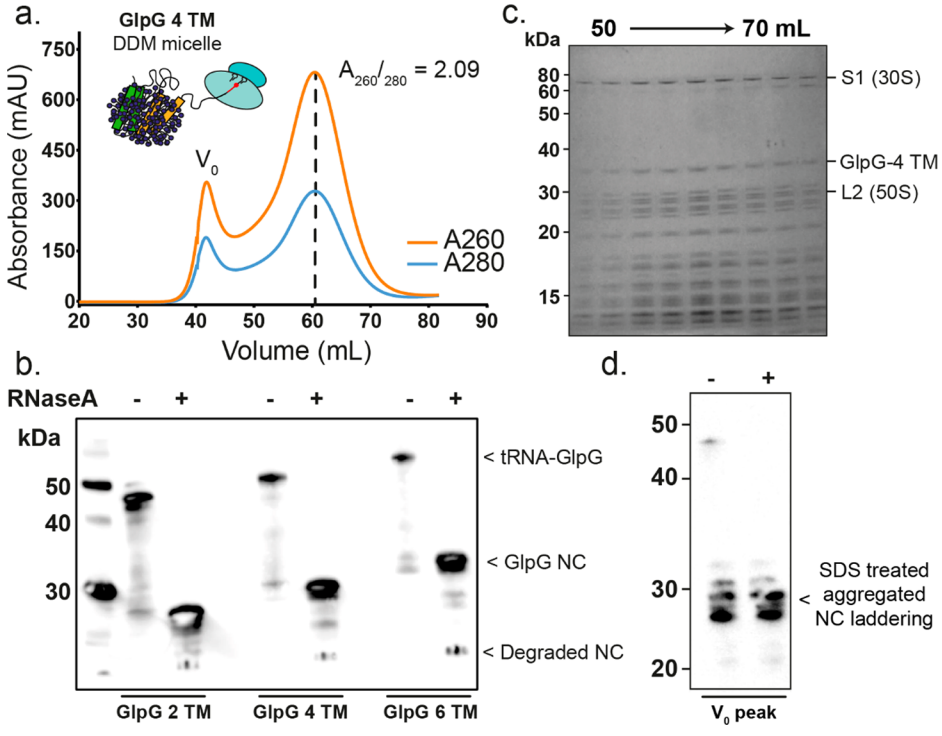

Figure 2. Purification of GlpG RNCs in DDM detergent micelles. (a) Representative SEC trace showing void and elution peaks at ∼60 mL for four-TM GlpG RNC. (b) DDM-solubilized GlpG RNCs were purified using IMAC followed by SEC using a 16/60 HiPrep Sephacryl S-400 column. Low-pH SDS−PAGE and Western blotting analysis of fractions under major elution peak show stalled ribosome complex before (−) and after (+) RNase A treatment [tRNA-GlpG and GlpG nascent chain (NC)-labeled bands respectively]; the stall is confirmed by a decrease in molecular weight as tRNA is digested. The size of these bands increases as the protein increases by two TM helices with each stall. (c) SDS−PAGE of fractions under the elution peak in panel a, showing characteristic 70S ribosome protein bands: the 30S S1 protein at ∼65 kDa, the 50S L2 protein at ∼30 kDa, and a selection of other ribosomal proteins below 30 kDa after Coomassie staining.[56] (d) Western blot analysis of a void peak from a four-TM GlpG RNC preparation in the DDM detergent. This peak appears to contain aggregated, released nascent chain. All Western blots were probed using a polyhistidine-HRP antibody.

https://dx.doi.org/10.1021/acs.biochem.0c00423
Biochemistry 2020, 59, 2764−2775

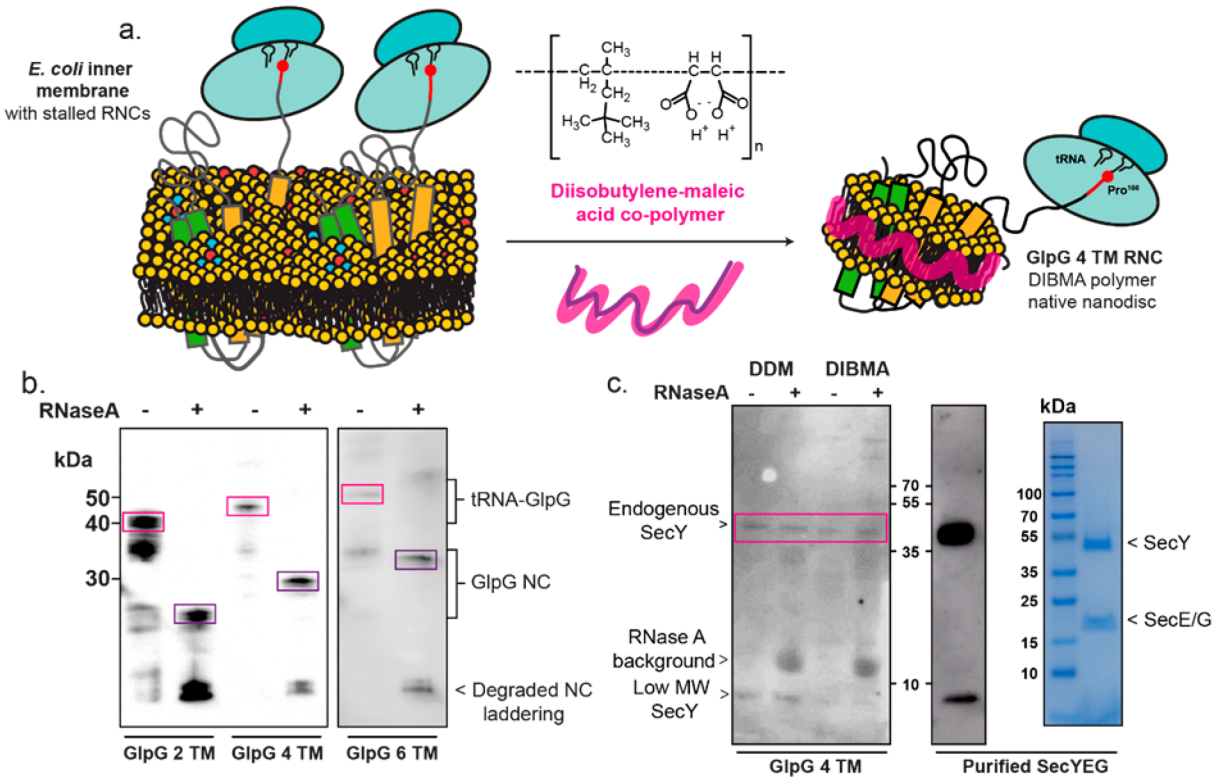

Figure 3. Preparation of GlpG RNCs in DIBMA nanodiscs shows evidence of co-purification with SecYEG. (a) Schematic of RNC DIBMA nanodisc preparation. *E. coli* inner membranes packed with membrane protein RNCs were subject to DIBMA solubilization to produce homogeneous RNC nanodiscs containing a native lipid environment. (b) GlpG RNC samples were solubilized with the DIBMA co-polymer and RNC DIBMA nanodiscs purified using IMAC followed by SEC. Arginine (0.2 M) was added to the SEC mobile phase to reduce the level of nonspecific aggregation of DIBMA nanodiscs with the resin of the 16/60 HiPrep Sephacryl S-400 size-exclusion column. Low-pH SDS−PAGE and Western blot analysis were used to assess the three RNC lengths from DIBMA preparations. Intact DIBMA-solubilized RNCs (pre-RNase A) for each stall length (two, four, and six TMs) are highlighted by pink boxes; released GlpG nascent chains due to RNase A treatment (+) are boxed in purple. Any unlabeled bands are identified as released, truncated, or aggregated GlpG caused by arginine-facilitated migration of the void peak into the SEC elution peak (see Figure S3c). All Western blots were probed using a polyhistidine-HRP antibody. (c) Evidence of endogenous SecYEG was detected within GlpG RNC samples prepared in the DDM detergent and DIBMA nanodiscs. Endogenous SecY was found to be present in samples before (−) and after (+) RNase A treatment (highlighted with a pink box, left panel). The low-molecular weight SecY band is characteristic of a C-terminal cleavage product.[62] Its 37 kDa band was confirmed by comparison with a Western blot (middle panel) and SDS−PAGE (right panel) of purified SecYEG, SecE and SecG co-migrating in this SDS−PAGE environment. All Western blots were probed using a monoclonal antibody for SecY.

GlpG was eluted with 100% buffer C and injected directly onto a Superdex 75 10/600 GL size-exclusion chromatography (SEC) column (GE Healthcare) equilibrated in buffer D [50 mM Tris (pH 7.4) at room temperature, 150 mM NaCl, 10% glycerol, and 0.025% (w/v) DDM]. Peak fractions that eluted from the SEC column containing GlpG were pooled and spin filtered before being flash-frozen and stored at −80 or −20 °C. SDS−PAGE and Western blotting, with an anti-histidine antibody, were used to assess GlpG purification.

EnzCheck Protease Activity Assay for GlpG. Detailed GlpG activity assay methods can be found in refs 21 and 46. Briefly, 5 μg/mL EnzCheck BODIPY-Casein substrate (ThermoScientific) was cleaved by 1 mg/mL GlpG overnight and in the dark at 4 °C in GlpG purification buffer D (see above). The resulting fluorescence that was emitted at 510 nm upon excitation with 480 nm light was recorded on a Horiba Fluoromax 4 instrument. This was a measure of the reduction of the level of self-quenching of BODIPY as casein is cleaved, indicative of GlpG protease activity. GlpG's activity was inhibited with the addition of 100 μM diisopropyl fluorophosphate (DFP).

Growth and Preparation of SecYEG. pBAD SecYEG was transformed into C43 cells and maintained with 100 μg/mL ampicillin. Overnight cultures of transformed cells were grown at 37 °C and used to seed 3 L of LB medium containing 100 μg/mL ampicillin. Cells were induced with 0.1% L-arabinose and grown until saturation was achieved. SecE (containing a C-terminal His_6 tag) is under the control of an arabinose promoter, and therefore, no IPTG is required for induction. Cells were harvested and suspended in 1× PBS with a cOmplete protease inhibitor tablet and stored at −20 °C until the day of use.

Cells were defrosted slowly and incubated with Benzonase nuclease before lysis using a constant systems cell disruptor at 25000 psi. The membrane fraction was harvested at 150000*g* and solubilized in 20 mM Tris (pH 8.0), 300 mM NaCl, 10% glycerol, 0.1 mM PMSF, 2% DDM, 20 mM imidazole, and an EDTA-free protease inhibitor tablet for 2 h at 4 °C. Insoluble material was removed with a 100000*g* centrifugation step, and the supernatant was loaded directly onto an AKTA Pure purification system.

The sample was passed over a Ni-NTA column at a rate of 0.5 mL/min for affinity purification of the SecYEG using a six-

https://dx.doi.org/10.1021/acs.biochem.0c00423
Biochemistry 2020, 59, 2764−2775

His tag. The trap was washed with 30 mL of the buffer described above before elution in 20 mM Tris (pH 8.0), 300 mM NaCl, 10% glycerol, 0.2 mM PMSF, 0.1% DDM, 1 mM 2-mercaptoethanol, and 500 mM imidazole. The eluate was immediately passed over a Superdex 16/600 column in 20 mM Tris (pH 8.0), 300 mM NaCl, 10% glycerol, 0.1 mM PMSF, and 0.1% DDM. Peak fractions were collected and concentrated using a 100 kDa concentrator if necessary and subsequently snap-frozen and stored at −70 °C until use.

RESULTS AND DISCUSSION

A Strategy for the Preparation of Polytopic α-Helical Protein RNCs. The *E. coli* rhomboid protease GlpG was used to benchmark our strategies for RNC generation. GlpG has six transmembrane-spanning α-helices and an N-terminal α-helix/β-sheet structured domain housing its catalytic dyad (denoted CytD), separated from the TM domain by a flexible linker, L_n. High-resolution structures of each domain exist, but not that of the full-length protein.[47−49]

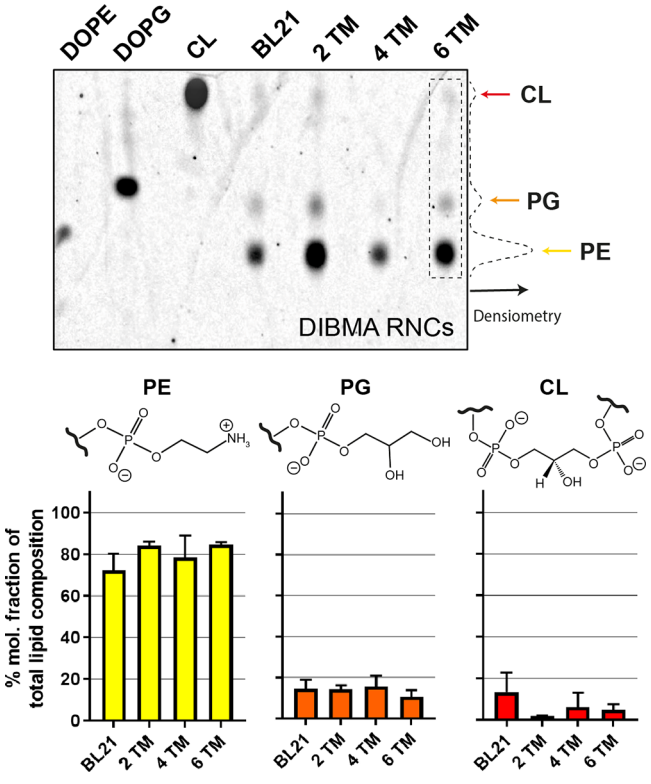

Figure 4. GlpG RNCs prepared in DIBMA nanodiscs contain native lipid compositions. DIBMA GlpG RNC samples and cell membranes, prepared from BL21 *E. coli* cells grown in minimal media, were subjected to Folch lipid extraction. Extractions were run alongside standards of DOPE, DOPG, and CL. A representative TLC plate from samples grown in MDG/EM9 media is shown. The three bar charts show a similar relative abundance of each lipid for each stall length (the 2 TM label denotes two-TM GlpG RNC extraction) as determined using densitometry analysis. The mean percent lipid composition and SD are plotted for three or more biological repeats for each stall length (see Materials and Methods). Phospholipid headgroups for phosphatidylethanolamine (PE), phosphatidylglycerol (PG), and cardiolipin (CL) are shown.

GlpG has become a model membrane protein for *in vitro* folding and stability work[21,38] and has been interrogated by chaotrope,[50] heating,[51] steric trapping,[52] or mechanical force.[53] These systems, however, do not truly represent the *in vivo* folding situation whereby mRNA is translated by the ribosome and protein forms and folds during chain elongation in unison with translation. More recently, surface-enhanced infrared absorption spectroscopy (SEIRAS) and IVTT systems were used to determine secondary structure folding of the GlpG nascent chain as it was translated by the ribosome and inserted into translocon-free MSP-based lipid nanodiscs.[20,21] This allowed time-resolved analysis of co-translational folding of GlpG for the first time but nonetheless lacked a native membrane lipid environment.

GlpG RNCs of varying nascent chain lengths were generated *in vivo* using the SecM stalling motif (^{150}FSTPVWISQA-QGIRAGP^{166}). An *E. coli* SecM arrest sequence[9,24] was cloned downstream of two, four, and six predicted TM helices (see Materials and Methods). Stalling positions were chosen on the basis of translocon-mediated MPEx hydropathy analysis[27] (Figure 1a,b), which describes the free energy required for a stretch of amino acids to partition into the membrane environment, taking into account not only the identity of the amino acid but also the TM segment length and the influence of flanking amino acids. To allow all TM regions of interest to be fully translated, the length of the ribosome tunnel was also taken into account, which has been approximated to accommodate ∼40 fully extended amino acids.[54] Hence, the final Pro^{166} stalling residue and the C-terminal end of the TM of interest were separated by 44 amino acids (including the SecM motif and linker residues).

To facilitate purification of *in vivo*-generated RNCs, a six-histidine affinity tag (His tag) was placed at the N-terminus of GlpG (Figure 1c). The introduction of the N-terminal tag did not affect protease activity when compared to a C-terminal construct (Figure S2a), or sorting to the membrane, and overexpression of these RNC constructs was found to be nontoxic to BL21 *E. coli* expression cells (Figure S2b). Additionally, we establish that *in vivo* biotinylation of the membrane protein nascent chain can be achieved through the incorporation of an Avi tag (see the Supporting Information and Figure S1). This expands the capability of our constructs for purification by biotin/avidin affinity chromatography and/or advanced biophysical interrogation.[29,30]

To assess the ability of the designed constructs to generate membrane protein RNCs, they were initially purified in detergent micelles following cell growth in both minimal and Luria-Bertani media. Cell membranes containing overexpressed GlpG RNCs were isolated and solubilized with *n*-dodecyl β-D-maltoside (DDM) detergent before purification with immobilized metal affinity chromatography (IMAC) and size-exclusion chromatography (SEC) (Figure 2a). Stalled nascent chains can be characterized by low-pH SDS−PAGE analysis, which preserves the nascent chain−tRNA ester bond supplying an increased shift in mass and a reduced rate of migration.[2] RNase A treatment digests the bound tRNA, leaving the stalled polypeptide. All three RNC constructs (two-, four-, and six-TM GlpG) eluted as two resolved peaks upon SEC (Figure 2a and Figure S2d); the void peak (V_0) was found to contain aggregates of the released nascent chain (observed by Western blotting) and aggregated 70S ribosomes (observed by Coomassie staining) (Figure 2d and Figure S2c). The major elution peak at ∼60 mL contained homogeneous GlpG RNCs as confirmed by low-pH SDS−PAGE and Western blotting (Figure 2b,c), with an A_{260}/A_{280} ratio of ∼2.1 signifying the presence of homogeneous 70S ribosomes.[41]

https://dx.doi.org/10.1021/acs.biochem.0c00423
Biochemistry 2020, 59, 2764−2775

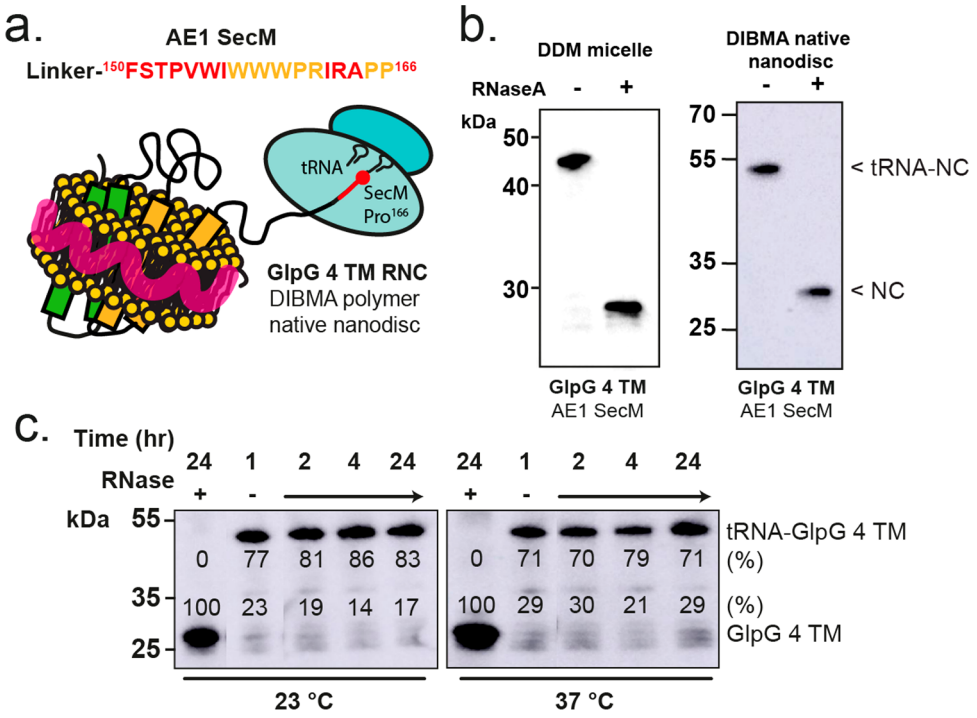

Figure 5. Arrest-enhanced SecM provides yields MP RNCs with greater stability, occupancy, and purity. (a) AE1 SecM sequence, with residues differing from the WT SecM sequence colored orange. (b) Low-pH SDS−PAGE and Western blotting analysis show that the AE1 RNC constructs are consistent with WT SecM for four-TM GlpG in both DDM and DIBMA, but the degree of spontaneously released nascent chain is significantly reduced (see Figures 2a and 3b). (c) AE1 SecM GlpG four-TM RNCs purified in DIBMA nanodiscs were heated at 23 and 37 °C for 24 h. Samples were taken and blotted after 1, 2, 4, and 24 h before low-pH SDS−PAGE and Western blotting analysis. The ratio between intact RNC (~50 kDa band, tRNA-GlpG 4 TM) and spontaneously released nascent chain (~30 kDa band, GlpG 4 TM) was calculated for each lane using the band density and ImageJ.[42] Percentages of intact and released are quoted next to the corresponding band. There was no significant release for each temperature from 1 to 24 h.

This purification strategy is faster than sucrose gradient preparations commonly used for RNC preparations,[2] with the shorter purification time being preferable for maintaining the integrity of membrane protein samples in detergent micelles.[55] However, the RNC constructs were also amenable to sucrose gradient purification post-IMAC (Figure S2e).

Low-intensity bands underneath the major GlpG construct bands were observed by Western blotting and attributed to small populations of truncated GlpG. This is commonly observed within preparations of RNCs by SecM-based stalling,[1,57] caused by digestion with remaining proteases during purification. Notably, when the GlpG constructs were released from the ribosome, they became more prone to degradation, suggesting that the constructs are stabilized and/or protected by the ribosome to protease digestion (Figure 2b).

Yields of RNC varied between nascent chain lengths when overexpressed and purified under identical conditions. Purified yields for the two-, four-, and six-TM constructs were ~30, 100, and 25 pmol/mL, respectively, based on the rRNA (A_{260}) content and assuming 100% ribosome/NC occupancy in DDM detergent. The individual yields may be linked to the extent of expected membrane force pulling of the different nascent chain lengths,[16,17,26] with an increased "insertion force" of some sequences reducing the stalling effect of SecM and in turn the quantity of stable RNCs obtained. MPEx analysis indicates that the four-TM construct is preceded by TM regions TM3 and TM4 that have the least favorable insertion energetics (Figure 1b). As a result, SecM stalling is effective and this is the highest-yield construct. On the contrary, the two- and six-TM constructs are preceded by TMs with much more favorable insertion energetics (lower-energy minima), which may lead to decreased RNC stalling stability and, therefore, the reduced yields observed.

The yields achieved for GlpG RNCs are sufficient for further structural and biochemical analyses but are around 100-fold lower than those previously quoted for small globular protein RNCs by Cabrita et al.[2] This is likely due to the toxic nature of overexpressing membrane proteins, caused in part by saturation of available SecYEG translocons.[58] Indeed, GlpG has been shown to insert into the *E. coli* inner membrane using SecYEG and YidC;[59] however, details of these interactions are currently unknown.[60]

Capturing Membrane Protein RNCs within DIBMA Nanodiscs. To capture RNCs in a native lipid surrounding, GlpG RNCs with two, four, and six TMs were isolated with DIBMA using a protocol similar to that for DDM but with some important modifications (Figure 3a and Figure S3ab). Isolated membranes were solubilized using DIBMA, which has a lower solubilization efficiency compared to that of the DDM detergent and SMA co-polymer. Higher divalent cation concentrations (in the presence of 10 mM Mg^{2+} or 7.5 mM Ca^{2+}) have been shown to improve DIBMA-meditated solubilization of *E. coli* membranes by up to 2-fold, through association and neutralization of the polymer's carboxylate groups.[35] To this end, the magnesium acetate concentration was increased in our membrane solubilization buffers from 6 to 12 mM. Solubilized membranes containing His-tagged GlpG RNCs were then batch bound to superaffinity Ni-NTA beads overnight at 4 °C to allow nickel−histidine coordination. This

https://dx.doi.org/10.1021/acs.biochem.0c00423
Biochemistry 2020, 59, 2764−2775

step was necessary as we found that DIBMA could interfere with nickel−histidine coordination,[9,10] reducing the level of the binding of the His tag to the Ni^{2+} resin; in contrast, DDM detergent preparations did not require long incubation times for adequate binding to occur.

Dynamic light scattering was used to assess the size and homogeneity of solubilized, IMAC-purified four-TM GlpG RNCs and gave a mean peak size of 10.5 nm, which is close to the value of 12.7 nm previously reported for full-length GlpG in DIBMA.[38] The average particle size z (which is the intensity-weighted mean hydrodynamic size of the ensemble) was determined to be 33.0 nm, suggestive of populations of ribosome-bound and unbound discs causing sample polydispersity (Figure S3d).

Affinity-purified DIBMA-solubilized GlpG RNCs were then subjected to SEC for further purification from protein-free DIBMA discs, released nascent chains, and aggregated RNCs. However, during SEC, the DIBMA polymer was found to interact with the Sephacryl S400 resin, which prevented its elution from the column. To counter this, 0.2 M arginine was added to the SEC buffer mobile phase to mitigate interactions of the protein disc with the resin and eliminate possible aggregation[61] (Figure S3c). With arginine present, the DIBMA nanodisc samples could now be resolved by SEC but with an elution behavior different from that found within DDM detergent preparations: the void peak disappeared, and the major peak shifted to a larger elution volume (Figure S3c). 70S ribosomal controls in the presence and absence of arginine in SEC buffer showed that this shift was caused by arginine, while the A_{260}/A_{280} ratios were unaffected.

Low-pH SDS−PAGE and Western blotting analysis showed that two-, four-, and six-TM RNCs within DIBMA nanodiscs (pink box) were successfully obtained (Figure 3b). However, the Western blot shows an increased rate of nascent chain release (purple box), particularly in the two-TM GlpG RNC, even before treatment with RNase A. We suggest these bands are released nascent chain, previously found as aggregates in the void peak in DDM preparations, which migrate into the major elution peak during SEC, which is caused by the inclusion of arginine in the mobile phase (Figure 3b and Figure S3c).

Sucrose gradients, employing a continuous 5 to 50% gradient, were used to eradicate released nascent chain artifacts caused by SEC arginine preparation of RNC DIBMA nanodiscs following IMAC purification (see Materials and Methods). The increased density of the lipid discs results in DIBMA nanodisc samples residing in the bottom fifth of the sucrose layer (Figure S3e), as has been shown previously for membrane-associated RNCs,[57] providing pure and homogeneous samples. This supports the idea that sucrose gradient purification is also a viable purification strategy for RNC DIBMA nanodisc samples (DIBMA samples being more stable than those in DDM).

The Endogenous SecYEG Translocon Associates with GlpG RNCs. To explore whether any SecYEG remained associated with GlpG RNCS, we probed the four-TM GlpG RNC purified in DDM and DIBMA nanodiscs for the presence of any endogenous Sec translocase machinery using a monoclonal SecY antibody.[62] SDS−PAGE and Western blot analysis revealed the presence of endogenous SecY (which has a blot intensity that is lower than that of overexpressed RNC) within both DDM and DIBMA samples (Figure 3c). This co-purification of SecY supports the idea that a GlpG RNC, Sec translocase interaction *in vivo* is maintained upon isolation in DDM or DIBMA.

DIBMA Captures Membrane Protein RNCs within a Native Lipid Environment. To ensure that the DIBMA polymer had solubilized GlpG RNCs within a native lipid environment, we assessed the lipid compositions using high-performance thin-layer chromatography (HPTLC). Purified RNC DIBMA nanodisc samples and cell membranes from non-induced cells, grown at the same temperature, were subject to Folch lipid extraction. The lipid identity and relative mole ratio of each observed lipid were then assessed using HPTLC analysis (Figure 4). The three major phospholipid types expected within the *E. coli* inner membrane are phosphatidylethanolamine (PE), phosphatidylglycerol (PG), and cardiolipin (CL). We found that all DIBMA GlpG RNC nanodiscs contained similar relative abundances of PE, PG, and CL and compared to the non-induced membrane extract when grown in MDG/EM9 media (Figure 4).

A small increase in the abundance of PE and a decrease in the abundance of CL were seen between uninduced BL21 cells and the GlpG RNC DIBMA preparations (especially for the two-TM GlpG construct). Lipid membrane solubilization by DIBMA is relatively unexplored, but these effects may arise from collision lipid transfer[63] or preferential solubilization by DIBMA or reflect the two-TM local lipid environment as previously shown with SMA.[64] When RNCs were grown in LB medium, neutral lipids were also found in addition to the expected phospholipid composition (Figure S4), as confirmed by iodine vapor and molybdenum blue staining.[45] This has also previously been observed in DIBMA nanodiscs of full-length GlpG.[38]

Taken together, we observed that DIBMA is capable of extracting MP RNCs within a composition akin to its native lipid bilayer.

An Enhanced SecM Arrest Sequence Dramatically Improves Membrane Protein RNC Stability. An enhanced arrest sequence (AE1) (^{150}FSTPVWIWWWPRIRAPP^{166})[26] was employed to improve the stability of RNCs and mitigate the release of the nascent chain during and after purification, thus enhancing RNC quality and longevity. Compared to WT SecM, the AE1 SecM sequence contains an additional proline at position 165 and a substituted stretch of tryptophan amino acids (Figure 5a), which forms more interactions with the ribosome exit tunnel and further occludes peptide bond formation in the PTC.[4]

Four-TM GlpG RNCs were prepared with the AE1 SecM stalling sequence in both DDM micelles and DIBMA nanodiscs, yielding samples of a quality higher than that achieved with WT SecM, as evidenced by negligible nascent chain release and degradation observed by Western blotting (Figure 5b). Improved nascent chain retention was also found for AE1 SecM RNCs, with only 12% spontaneous release of nascent chain from AE1 SecM RNCs observed over 24 h at 23 °C, compared to 35% for WT SecM, for DDM purified samples under the same conditions (IMAC and SEC purification) (Figure S5a). These percentages were estimated by using densitometry analysis at each time point and calculating the relative ratios of tRNA-bound four-TM GlpG and naturally released four-TM nascent chain. Moreover, four-TM GlpG RNCs containing WT SecM released 48% of their nascent chain upon only one freeze−thaw cycle, whereas AE1 SecM released only 18% (Figure S5c).

https://dx.doi.org/10.1021/acs.biochem.0c00423
Biochemistry 2020, 59, 2764−2775

Four-TM GlpG AE1 SecM RNCs, prepared in DIBMA (by IMAC and sucrose gradient purification), were incredibly stable; no significant release was found after 24 h at both 23 and 37 °C (Figure 5c). Furthermore, these samples were able to withstand at least six freeze−thaw cycles with no significant release of the nascent chain (Figure S5b).

We also estimated the fraction of ribosomes in the samples that contain bound nascent chain to understand purified RNC occupancy. Occupancy was calculated by blotting the known A_{260}-derived concentration of each RNC sample (where 1 A_{260} = 24 pmol/mL) against full-length GlpG standards (Figure S5c) and calculating the picomoles of GlpG NC for the tRNA-bound band.[2] There was an increase in occupancy of AE1 SecM RNCs in DDM (85% occupancy) compared to that of WT SecM RNC (75% occupancy). An occupancy of 75% was determined for AE1 SecM RNC in DIBMA; however, there is no significant release of this DIBMA nascent chain compared to that of DDM detergent samples (Figure S5c). This signifies that incorporation of the AE1 sequence leads to a significant increase in RNC stability, which will aid future structural, biochemical, and biophysical analysis.

CONCLUSIONS

We demonstrate that pure, stable RNCs of different nascent chain lengths can be prepared for a polytopic α-helical integral membrane protein, in both detergent micelle and native lipid surroundings. This work advances membrane protein RNC preparations by establishing that (1) SecM stalling can successfully stall a polytopic α-helical MP at various points throughout its synthesis to yield stable RNCs for structural interrogation, thus allowing folding of the full chain to be probed as opposed to single, short TM constructs previously investigated, (2) RNC constructs are tolerant to different purification tags, such as His and Avi tags, enabling diverse purification and experimental strategies to be devised, (3) the nascent chain is maintained within a lipid bilayer comprised of its cellular lipid mixtures rather than synthetic lipids, and (4) RNCs are extracted directly from native membranes, escaping reconstitution of isolated RNCs prepared in non-native environments and permitting co-purification of endogenous chaperones, such as the SecYEG translocon.

Overall, we reveal that homogeneous membrane protein RNCs can be captured within a native lipid environment using DIBMA native nanodisc technology. These samples are stable for the time frames and conditions required for future biochemical and structural studies.[65,66] *In vivo*-formed membrane protein RNCs generated here provide snapshots of co-translational folding, paused at various nascent chain lengths, and are a stepping stone toward studying the structure and dynamics of co-translational membrane protein folding in an increasingly more *in vivo* context.

ASSOCIATED CONTENT

Supporting Information

The Supporting Information is available free of charge at https://pubs.acs.org/doi/10.1021/acs.biochem.0c00423.

Discussion of *in vivo* biotinylation procedures and Figures S1−S5 (PDF)

Accession Codes

UniProtKB codes: GLPG, P09391; SECY, P0AGA2; SECE, P0AG96; SECG, P0AG99. Small ribosomal subunits (30S): RS1, P0AG67; RS2, P0A7V0; RS3, P0A7V3; RS4, P0A7V8; RS5, P0A7W1; RS6, P02358; RS7, P02359; RS8, P0A7W7; RS9, P0A7X3; RS10, P0A7R5; RS11, P0A7R9; RS12, P0A7S3; RS13, P0A7S9; RS14, P0AG59; RS15, P0ADZ4; RS16, P0A7T3; RS17, P0AG63; RS18, P0A7T7; RS19, P0A7U3; RS20, P0A7U7; RS21, P68681; RS22, C8U8F3. Large ribosomal subunits (50S): RL1, P0A7L0; RL2, P60422; RL3, P60438; RL4, P60723; RL5, P62399; RL6, P0AG55; RL7, P0A7K2; RL9, P0A7R1; RL10, P0A7J3; RL11, P0A7J7; RL13, P0AA10; RL14, P0ADY3; RL15, P02413; RL16, P0ADY7; RL17, P0AG44; RL18, P0C018; RL19, B1LPB3; RL20, P0A7L3; RL21, P0AG48; RL22, P61175; RL23, P0ADZ0; RL24, P60624; RL25, P68919; RL27, P0A7M0; RL28, P0A7M2; RL29, P0A7M6; RL30, P0AG51; RL31, P0A7M9; RL32, C4ZS29; RL33, P0A7N9; RL34, P0A7P6; RL35, P0A7Q2; RL36, P0A7Q7.

AUTHOR INFORMATION

Corresponding Authors

Paula J. Booth − *King's College London, Department of Chemistry, London SE1 1DB, U.K.*; Email: paula.booth@kcl.ac.uk

Eamonn Reading − *King's College London, Department of Chemistry, London SE1 1DB, U.K.*; orcid.org/0000-0001-8219-0052; Email: eamonn.reading@kcl.ac.uk

Authors

Grant A. Pellowe − *King's College London, Department of Chemistry, London SE1 1DB, U.K.*; orcid.org/0000-0003-4314-5261

Heather E. Findlay − *King's College London, Department of Chemistry, London SE1 1DB, U.K.*

Karen Lee − *King's College London, Department of Chemistry, London SE1 1DB, U.K.*

Tim M. Gemeinhardt − *King's College London, Department of Chemistry, London SE1 1DB, U.K.*

Laura R. Blackholly − *King's College London, Department of Chemistry, London SE1 1DB, U.K.*

Complete contact information is available at: https://pubs.acs.org/10.1021/acs.biochem.0c00423

Author Contributions

G.A.P., E.R., and P.J.B. designed the research. G.A.P., H.E.F., K.L., T.M.G., and E.R. performed all experiments and analyses, except for SecYEG preparation, which was performed by L.R.B. E.R. and P.J.B. supervised the project. G.A.P., E.R., and P.J.B. wrote the manuscript with input from the other authors.

Funding

This work was supported by a BBSRC Future Leader Fellowship (BB/N011201/1) and a UKRI Future Leaders Fellowship (MR/S015426/1) to E.R., with support by the Erasmus+ programme of the European Union to T.M.G., an ERC Advanced Grant (294342) and a Wellcome Trust Investigator Award (214259/Z/18/Z) to P.J.B., and a King's College London Ph.D. studentship to G.A.P.

Notes

The authors declare no competing financial interest.

ACKNOWLEDGMENTS

The authors thank Prof. Ian Collinson at the University of Bristol for the generous donation of the pBAD-SecYEG plasmid and the monoclonal mouse SecY antibody for endogenous SecYEG detection. The authors also thank Prof.

Bernd Bukau and Dr. Guenter Kramer for providing plasmids containing SecM genes.

REFERENCES

(1) Cabrita, L. D., Hsu, S. T., Launay, H., Dobson, C. M., and Christodoulou, J. (2009) Probing ribosome-nascent chain complexes produced in vivo by NMR spectroscopy. *Proc. Natl. Acad. Sci. U. S. A. 106*, 22239−22244.
(2) Cassaignau, A. M., Launay, H. M., Karyadi, M. E., Wang, X., Waudby, C. A., Deckert, A., Robertson, A. L., Christodoulou, J., and Cabrita, L. D. (2016) A strategy for co-translational folding studies of ribosome-bound nascent chain complexes using NMR spectroscopy. *Nat. Protoc. 11*, 1492−1507.
(3) Waudby, C. A., Launay, H., Cabrita, L. D., and Christodoulou, J. (2013) Protein folding on the ribosome studied using NMR spectroscopy. *Prog. Nucl. Magn. Reson. Spectrosc. 74*, 57−75.
(4) Bischoff, L., Wickles, S., Berninghausen, O., van der Sluis, E. O., and Beckmann, R. (2014) Visualization of a polytopic membrane protein during SecY-mediated membrane insertion. *Nat. Commun. 5*, 4103.
(5) Kater, L., Frieg, B., Berninghausen, O., Gohlke, H., Beckmann, R., and Kedrov, A. (2019) Partially inserted nascent chain unzips the lateral gate of the Sec translocon. *EMBO Rep. 20*, No. e48191.
(6) Seidelt, B., Innis, C. A., Wilson, D. N., Gartmann, M., Armache, J. P., Villa, E., Trabuco, L. G., Becker, T., Mielke, T., Schulten, K., Steitz, T. A., and Beckmann, R. (2009) Structural insight into nascent polypeptide chain-mediated translational stalling. *Science 326*, 1412−1415.
(7) Woolhead, C. A., McCormick, P. J., and Johnson, A. E. (2004) Nascent Membrane and Secretory Proteins Differ in FRET-Detected Folding Far inside the Ribosome and in Their Exposure to Ribosomal Proteins. *Cell 116*, 725−736.
(8) Hoffmann, A., Merz, F., Rutkowska, A., Zachmann-Brand, B., Deuerling, E., and Bukau, B. (2006) Trigger factor forms a protective shield for nascent polypeptides at the ribosome. *J. Biol. Chem. 281*, 6539−6545.
(9) Rutkowska, A., Beerbaum, M., Rajagopalan, N., Fiaux, J., Schmieder, P., Kramer, G., Oschkinat, H., and Bukau, B. (2009) Large-scale purification of ribosome-nascent chain complexes for biochemical and structural studies. *FEBS Lett. 583*, 2407−2413.
(10) Schaffitzel, C., and Ban, N. (2007) Generation of ribosome nascent chain complexes for structural and functional studies. *J. Struct. Biol. 158*, 463−471.
(11) Schulze, R. J., Komar, J., Botte, M., Allen, W. J., Whitehouse, S., Gold, V. A., Lycklama a Nijeholt, J. A., Huard, K., Berger, I., Schaffitzel, C., and Collinson, I. (2014) Membrane protein insertion and proton-motive-force-dependent secretion through the bacterial holo-translocon SecYEG-SecDF-YajC-YidC. *Proc. Natl. Acad. Sci. U. S. A. 111*, 4844−4849.
(12) Harris, N. J., Charalambous, K., Findlay, H. E., and Booth, P. J. (2018) Lipids modulate the insertion and folding of the nascent chains of alpha helical membrane proteins. *Biochem. Soc. Trans. 46*, 1355−1366.
(13) Findlay, H. E., and Booth, P. J. (2017) The folding, stability and function of lactose permease differ in their dependence on bilayer lipid composition. *Sci. Rep. 7*, 13056.
(14) Bogdanov, M., Dowhan, W., and Vitrac, H. (2014) Lipids and topological rules governing membrane protein assembly. *Biochim. Biophys. Acta, Mol. Cell Res. 1843*, 1475−1488.
(15) Kuruma, Y., and Ueda, T. (2015) The PURE system for the cell-free synthesis of membrane proteins. *Nat. Protoc. 10*, 1328−1344.
(16) Ismail, N., Hedman, R., Linden, M., and von Heijne, G. (2015) Charge-driven dynamics of nascent-chain movement through the SecYEG translocon. *Nat. Struct. Mol. Biol. 22*, 145−149.
(17) Ismail, N., Hedman, R., Schiller, N., and von Heijne, G. (2012) A biphasic pulling force acts on transmembrane helices during translocon-mediated membrane integration. *Nat. Struct. Mol. Biol. 19*, 1018−1022.
(18) Dale, H., Angevine, C. M., and Krebs, M. P. (2000) Ordered membrane insertion of an archaeal opsin in vivo. *Proc. Natl. Acad. Sci. U. S. A. 97*, 7847−7852.
(19) Dale, H., and Krebs, M. P. (1999) Membrane insertion kinetics of a protein domain in vivo. The bacterioopsin n terminus inserts co-translationally. *J. Biol. Chem. 274*, 22693−22698.
(20) Pellowe, G. A., and Booth, P. J. (2020) Structural insight into co-translational membrane protein folding. *Biochim. Biophys. Acta, Biomembr. 1862*, 183019.
(21) Harris, N. J., Reading, E., Ataka, K., Grzegorzewski, L., Charalambous, K., Liu, X., Schlesinger, R., Heberle, J., and Booth, P. J. (2017) Structure formation during translocon-unassisted co-translational membrane protein folding. *Sci. Rep. 7*, 8021.
(22) Ataka, K., Stripp, S. T., and Heberle, J. (2013) Surface-enhanced infrared absorption spectroscopy (SEIRAS) to probe monolayers of membrane proteins. *Biochim. Biophys. Acta, Biomembr. 1828*, 2283−2293.
(23) Evans, M. S., Ugrinov, K. G., Frese, M. A., and Clark, P. L. (2005) Homogeneous stalled ribosome nascent chain complexes produced in vivo or in vitro. *Nat. Methods 2*, 757−762.
(24) Nakatogawa, H., and Ito, K. (2002) The Ribosomal Exit Tunnel Functions as a Discriminating Gate. *Cell 108*, 629−636.
(25) Bhushan, S., Hoffmann, T., Seidelt, B., Frauenfeld, J., Mielke, T., Berninghausen, O., Wilson, D. N., and Beckmann, R. (2011) SecM-stalled ribosomes adopt an altered geometry at the peptidyl transferase center. *PLoS Biol. 9*, No. e1000581.
(26) Cymer, F., Hedman, R., Ismail, N., and von Heijne, G. (2015) Exploration of the arrest peptide sequence space reveals arrest-enhanced variants. *J. Biol. Chem. 290*, 10208−10215.
(27) Snider, C., Jayasinghe, S., Hristova, K., and White, S. H. (2009) MPEx: a tool for exploring membrane proteins. *Protein Sci. 18*, 2624−2628.
(28) Marinko, J. T., Huang, H., Penn, W. D., Capra, J. A., Schlebach, J. P., and Sanders, C. R. (2019) Folding and Misfolding of Human Membrane Proteins in Health and Disease: From Single Molecules to Cellular Proteostasis. *Chem. Rev. 119*, 5537−5606.
(29) Goldman, D. H., Kaiser, C. M., Milin, A., Righini, M., Tinoco, I., Jr., and Bustamante, C. (2015) Ribosome. Mechanical force releases nascent chain-mediated ribosome arrest in vitro and in vivo. *Science 348*, 457−460.
(30) Kaiser, C. M., Goldman, D. H., Chodera, J. D., Tinoco, I., Jr., and Bustamante, C. (2011) The ribosome modulates nascent protein folding. *Science 334*, 1723−1727.
(31) Oluwole, A. O., Danielczak, B., Meister, A., Babalola, J. O., Vargas, C., and Keller, S. (2017) Solubilization of Membrane Proteins into Functional Lipid-Bilayer Nanodiscs Using a Diisobutylene/Maleic Acid Copolymer. *Angew. Chem., Int. Ed. 56*, 1919−1924.
(32) Oluwole, A. O., Klingler, J., Danielczak, B., Babalola, J. O., Vargas, C., Pabst, G., and Keller, S. (2017) Formation of Lipid-Bilayer Nanodiscs by Diisobutylene/Maleic Acid (DIBMA) Copolymer. *Langmuir 33*, 14378−14388.
(33) Simon, K. S., Pollock, N. L., and Lee, S. C. (2018) Membrane protein nanoparticles: the shape of things to come. *Biochem. Soc. Trans. 46*, 1495−1504.
(34) Nierhaus, K. H. (2014) Mg2+, K+, and the ribosome. *J. Bacteriol. 196*, 3817−3819.
(35) Danielczak, B., Meister, A., and Keller, S. (2019) Influence of Mg(2+) and Ca(2+) on nanodisc formation by diisobutylene/maleic acid (DIBMA) copolymer. *Chem. Phys. Lipids 221*, 30−38.
(36) Denisov, I. G., and Sligar, S. G. (2017) Nanodiscs in Membrane Biochemistry and Biophysics. *Chem. Rev. 117*, 4669−4713.
(37) Ravula, T., Hardin, N. Z., and Ramamoorthy, A. (2019) Polymer nanodiscs: Advantages and limitations. *Chem. Phys. Lipids 219*, 45−49.
(38) Barniol-Xicota, M., and Verhelst, S. H. L. (2018) Stable and Functional Rhomboid Proteases in Lipid Nanodiscs by Using Diisobutylene/Maleic Acid Copolymers. *J. Am. Chem. Soc. 140*, 14557−14561.

https://dx.doi.org/10.1021/acs.biochem.0c00423
Biochemistry 2020, 59, 2764−2775

(39) Gulamhussein, A. A., Uddin, R., Tighe, B. J., Poyner, D. R., and Rothnie, A. J. (2020) A comparison of SMA (styrene maleic acid) and DIBMA (di-isobutylene maleic acid) for membrane protein purification. *Biochim. Biophys. Acta, Biomembr. 1862*, 183281.
(40) Becker, M., Gzyl, K. E., Altamirano, A. M., Vuong, A., Urbahn, K., and Wieden, H. J. (2012) The 70S ribosome modulates the ATPase activity of Escherichia coli YchF. *RNA Biol. 9*, 1288−1301.
(41) Hill, W. E., Rossetti, G. P., and Van Holde, K. E. (1969) Physical studies of ribosomes from Escherichia coli. *J. Mol. Biol. 44*, 263−277.
(42) Schneider, C. A., Rasband, W. S., and Eliceiri, K. W. (2012) NIH Image to ImageJ: 25 years of image analysis. *Nat. Methods 9*, 671−675.
(43) Folch, J., Lees, M., and Sloane Stanley, G. H. (1957) A simple method for the isolation and purification of total lipides from animal tissues. *J. Biol. Chem. 226*, 497−509.
(44) Churchward, M. A., Brandman, D. M., Rogasevskaia, T., and Coorssen, J. R. (2008) Copper (II) sulfate charring for high sensitivity on-plate fluorescent detection of lipids and sterols: quantitative analyses of the composition of functional secretory vesicles. *J. Chem. Biol. 1*, 79−87.
(45) Dynska-Kukulska, K., Ciesielski, W., and Zakrzewski, R. (2013) The use of a new, modified Dittmer-Lester spray reagent for phospholipid determination by the TLC image analysis technique. *Biomed. Chromatogr. 27*, 458−465.
(46) Reading, E., Hall, Z., Martens, C., Haghighi, T., Findlay, H., Ahdash, Z., Politis, A., and Booth, P. J. (2017) Interrogating Membrane Protein Conformational Dynamics within Native Lipid Compositions. *Angew. Chem., Int. Ed. 56*, 15654−15657.
(47) Brooks, C. L., and Lemieux, M. J. (2013) Untangling structure-function relationships in the rhomboid family of intramembrane proteases. *Biochim. Biophys. Acta, Biomembr. 1828*, 2862−2872.
(48) Sherratt, A. R., Blais, D. R., Ghasriani, H., Pezacki, J. P., and Goto, N. K. (2012) Activity-based protein profiling of the Escherichia coli GlpG rhomboid protein delineates the catalytic core. *Biochemistry 51*, 7794−7803.
(49) Vinothkumar, K. R. (2011) Structure of rhomboid protease in a lipid environment. *J. Mol. Biol. 407*, 232−247.
(50) Paslawski, W., Lillelund, O. K., Kristensen, J. V., Schafer, N. P., Baker, R. P., Urban, S., and Otzen, D. E. (2015) Cooperative folding of a polytopic alpha-helical membrane protein involves a compact N-terminal nucleus and nonnative loops. *Proc. Natl. Acad. Sci. U. S. A. 112*, 7978−7983.
(51) Baker, R. P., and Urban, S. (2012) Architectural and thermodynamic principles underlying intramembrane protease function. *Nat. Chem. Biol. 8*, 759−768.
(52) Guo, R., Gaffney, K., Yang, Z., Kim, M., Sungsuwan, S., Huang, X., Hubbell, W. L., and Hong, H. (2016) Steric trapping reveals a cooperativity network in the intramembrane protease GlpG. *Nat. Chem. Biol. 12*, 353−360.
(53) Min, D., Jefferson, R. E., Bowie, J. U., and Yoon, T. Y. (2015) Mapping the energy landscape for second-stage folding of a single membrane protein. *Nat. Chem. Biol. 11*, 981−987.
(54) Jha, S., and Komar, A. A. (2011) Birth, life and death of nascent polypeptide chains. *Biotechnol. J. 6*, 623−640.
(55) Seddon, A. M., Curnow, P., and Booth, P. J. (2004) Membrane proteins, lipids and detergents: not just a soap opera. *Biochim. Biophys. Acta, Biomembr. 1666*, 105−117.
(56) Dzionara, M., Kaltschmidt, E., and Wittmann, H. G. (1970) Ribosomal proteins. 8. Molecular weights of isolated ribosomal proteins of Escherichia coli. *Proc. Natl. Acad. Sci. U. S. A. 67*, 1909−1913.
(57) Bercovich-Kinori, A., and Bibi, E. (2015) Co-translational membrane association of the Escherichia coli SRP receptor. *J. Cell Sci. 128*, 1444−1452.
(58) Schlegel, S., Rujas, E., Ytterberg, A. J., Zubarev, R. A., Luirink, J., and de Gier, J. W. (2013) Optimizing heterologous protein production in the periplasm of E. coli by regulating gene expression levels. *Microb. Cell Fact. 12*, 24.
(59) Schibich, D., Gloge, F., Pohner, I., Bjorkholm, P., Wade, R. C., von Heijne, G., Bukau, B., and Kramer, G. (2016) Global profiling of SRP interaction with nascent polypeptides. *Nature 536*, 219−223.
(60) Komar, J., Alvira, S., Schulze, R. J., Martin, R., Lycklama a Nijeholt, J. A., Lee, S. C., Dafforn, T. R., Deckers-Hebestreit, G., Berger, I., Schaffitzel, C., and Collinson, I. (2016) Membrane protein insertion and assembly by the bacterial holo-translocon SecYEG-SecDF-YajC-YidC. *Biochem. J. 473*, 3341−3354.
(61) Ejima, D., Yumioka, R., Arakawa, T., and Tsumoto, K. (2005) Arginine as an effective additive in gel permeation chromatography. *J. Chromatogr A 1094*, 49−55.
(62) Whitehouse, S., Gold, V. A., Robson, A., Allen, W. J., Sessions, R. B., and Collinson, I. (2012) Mobility of the SecA 2-helix-finger is not essential for polypeptide translocation via the SecYEG complex. *J. Cell Biol. 199*, 919−929.
(63) Danielczak, B., and Keller, S. (2018) Collisional lipid exchange among DIBMA-encapsulated nanodiscs (DIBMALPs). *Eur. Polym. J. 109*, 206−213.
(64) Teo, A. C. K., Lee, S. C., Pollock, N. L., Stroud, Z., Hall, S., Thakker, A., Pitt, A. R., Dafforn, T. R., Spickett, C. M., and Roper, D. I. (2019) Analysis of SMALP co-extracted phospholipids shows distinct membrane environments for three classes of bacterial membrane protein. *Sci. Rep. 9*, 1813.
(65) Parmar, M., Rawson, S., Scarff, C. A., Goldman, A., Dafforn, T. R., Muench, S. P., and Postis, V. L. G. (2018) Using a SMALP platform to determine a sub-nm single particle cryo-EM membrane protein structure. *Biochim. Biophys. Acta, Biomembr. 1860*, 378−383.
(66) Reading, E. (2019) Assessing Membrane Protein Structural Dynamics within Lipid Nanodiscs. *Trends Biochem. Sci. 44*, 989−990.

https://dx.doi.org/10.1021/acs.biochem.0c00423
Biochemistry 2020, 59, 2764−2775